Reorganization of rich clubs in functional brain networks of dementia with Lewy bodies and Alzheimer's disease

Wen-ying Ma [a,1], Qun Yao [a,1], Guan-jie Hu [b], Hong-lin Ge [b], Chen Xue [c], Ying-ying Wang [a], Yi-xin Yan [a], Chao-yong Xiao [c], Jing-Ping Shi [a,e,*], Jiu Chen [d,e,*]

[a] Department of Neurology, Affiliated Nanjing Brain Hospital, Nanjing Medical University, Nanjing, Jiangsu 210029, China
[b] Department of Neurosurgery, Affiliated Nanjing Brain Hospital, Nanjing Medical University, Nanjing, Jiangsu 210029, China
[c] Department of Radiology, Affiliated Nanjing Brain Hospital, Nanjing Medical University, Nanjing, Jiangsu 210029, China
[d] Institute of Neuropsychiatry, Affiliated Nanjing Brain Hospital, Nanjing Medical University, Nanjing, Jiangsu 210029, China
[e] Institute of Brain Functional Imaging, Nanjing Medical University, Nanjing, Jiangsu 210029, China

ARTICLE INFO

ABSTRACT

The purpose of this study was to reveal the patterns of reorganization of rich club organization in brain functional networks in dementia with Lewy bodies (DLB) and Alzheimer's disease (AD). The study found that the rich club node shifts from sensory/somatomotor network to fronto-parietal network in DLB. For AD, the rich club nodes switch between the temporal lobe with obvious structural atrophy and the frontal lobe, parietal lobe and cerebellum with relatively preserved structure and function. In addition, compared with healthy controls, rich club connectivity was enhanced in the DLB and AD groups. The connection strength of DLB patients was related to cognitive assessment. In conclusion, we revealed the different functional reorganization patterns of DLB and AD. The conversion and redistribution of rich club members may play a causal role in disease-specific outcomes. It may be used as a potential biomarker to provide more accurate prevention and treatment strategies.

1. Introduction

Dementia with Lewy bodies (DLB) is a progressive dementia characterized by cognitive fluctuations, recurrent hallucinations, rapid eye movement sleep behavior disorder, and spontaneous Parkinson's disease (McKeith et al., 2017). Alzheimer's disease (AD) is the most common type of dementia accounting for 50% to 70% (McKeith et al., 2007). Although a large number of previous studies have established criteria for the clinical differentiation of DLB from AD (McKeith et al., 2005; McKeith et al., 1996). However, in some cases, it remains difficult to distinguish DLB from AD due to the commonality and overlap of clinical and neuropathological features (McKeith et al., 1994). These trends encourage research into the understanding of the etiological mechanisms of these two diseases, which is important to improve diagnostic accuracy, as well as to provide potential specific targets for treatment and prevention.

With the development of various neuroimaging techniques, the functional activity patterns of the brain in different disease phenotypes

have been used to understand the mechanism of occurrence and development of various diseases. As we all know, the human brain is a network of connections that supports sophisticated communication between brain regions. Hundreds of billions of closely connected neurons send out various signals, which are disseminated, transformed and processed through trillions of synapses (Daianu et al., 2016). Resting-state functional magnetic resonance imaging (RS-fMRI) analysis provides a noninvasive method to describe the reproducibility of macro functional networks. Research has found that some of these brain regions play a central role in the entire brain network, known as "brain hubs". They participate in multiple communities across the overall network, with the characteristics of high degree, low clustering, short path length and high centrality (Sporns et al., 2007; van den Heuvel et al., 2010). The "rich club" phenomenon refers to the fact that in a network, the connections between hubs tend to be closer than those between lower-level nodes (van den Heuvel and Sporns, 2011). Recent work applying this concept to healthy human brains has shown that both structural and functional networks do indeed exhibit robust rich club organizations. It is suggested that rich club organization may be a key topological property of healthy brains (van den Heuvel and Sporns, 2011). As a high-capacity central core, the rich club connection plays a crucial role in the global integration of neural information in various brain regions. Disconnection within the rich clubs has a significant effect on cognition, emotion and behavior (Yan et al., 2018).

Recent studies have shown that connections between rich clubs are affected in several mental disorders associated with cognitive and affective processing disorders, including schizophrenia, attention-deficit/hyperactivity disorder and autism spectrum disorders (van den Heuvel et al., 2013; Ray et al., 2014). The destruction of rich club attributes was found to be related to the decrease of brain communication level and global integration ability, which involves emotional and behavioral regulation (Collin et al., 2014; Collin et al., 2014). Some studies have reported that the lesion distribution of AD patients from preclinical stage to dementia stage were mainly concentrated in rich club connection (Crossley et al., 2014; Buckner et al., 2009; Dai et al., 2015; Brier et al., 2014; Shu et al., 2018). However, Daianu and his colleagues found that network disruption were dominant in peripheral network components in d-AD patients and less evident in mild cognitive impairment (MCI) patients (Daianu et al., 2015). Although the research on AD rich club organization has made progress, the results are inconsistent to some extent. However, the research on the organizational characteristics of DLB functional network using "rich club" has yet to be examined.

In addition, although the diagnostic criteria of DLB do not overlap with the diagnostic framework of AD. However, clinically, patients with AD can also have hallucinations, sleep disorders and other mental behavioral symptoms (Zhao et al., 2016), and patients with DLB often have prominent or persistent memory impairment as the disease progresses (Gu et al., 2018). Pathological studies have confirmed that DLB is often accompanied by AD-like pathology (Walker et al., 2015; Ruffmann et al., 2016), and Lewy bodies, the core pathological features of DLB, also are common in some early-onset familial AD cases and neuropathological changes of moderate to severe AD (Robinson et al., 2020; Montine et al., 2012). In order to determine whether certain common behavioral patterns are the result of similar functional neurophysiology, and to better assess which brain network organizational characteristics are affected by disease specific, a comparison between the two diseases in the same study is necessary. Although some scholars have reported significant differences in global network measurements between DLB and AD. For example, compared with Healthy controls (HC), AD showed lower small-worldness and global efficiency, while DLB showed higher levels of these indicators (Peraza et al., 2015). The results suggest divergent brain network organization in patients with AD and DLB. Unfortunately, there is no direct comparison between AD and DLB in the connection of rich clubs, so it is not clear whether they actually differ in terms of Rich Club.

The purpose of this study was to reveal the destruction and reorganization characteristics of rich club hubs in patients with AD and DLB. We first constructed a series of functional networks and defined specific brain rich club nodes in each group. Then the spatial location and network distribution differences of rich club nodes in each group are further evaluated. In addition, the change trend of nodal degree among the three groups was discussed quantitatively from the perspective of whole brain nodes. We hypothesize that the spatial location and network distribution of rich club nodes of these two dementia may be disturbed. The abnormal rich clubs might be related to structural atrophy and network abnormalities found in AD and DLB patients in previous studies.

2. Materials and methods

2.1. Participants

From May 2015 to September 2020, a total of 31 DLB patients, 42 AD patients and 34 HCs were recruited to the Affiliated Brain Hospital of Nanjing Medical University. Among them, 7 AD patients, 1 DLB patient and 1 HC patient were excluded because of excessive head movement (cumulative head motion > 3.0° or 3 mm, or mean FD Jenkinson > 0.2). In addition, 1 AD patient with poor registration effect was excluded. Finally, 30 DLB patients (mean age, 67.43 ± 5.32 years; 17 male), 34 AD patients (mean age, 65.88 ± 8.26 years; 14 male), and 33 HC (mean age, 64.94 ± 9.39 years; 15 male) were included in this study. Clinical diagnosis was made by two independent neurologists.

The inclusion criteria for HC were: 1) no abnormalities in cognitive performance, 2) no complaints of memory impairment, 3) Clinical Dementia Rating (CDR) score = 0 (Gu et al., 2018), and 4) matched with DLB and AD groups in age and gender. The inclusion criteria for DLB were based on the McKeith's criteria for probable DLB (McKeith et al., 2017; McKeith et al., 2005). All DLB patients suffered from two or more of the following core symptoms as follows: fluctuating cognition, recurrent visual hallucinations, rapid eye movement sleep behavior disorder, and spontaneous parkinsonism. The diagnosis of AD was made according to the criteria for probable AD of National Institute on Aging-Alzheimer's Association working group (McKhann et al., 2011). Subjects with a history of brain injury, other central nervous system disorders, severe medical conditions, and magnetic resonance imaging (MRI) contraindications were excluded in all groups. The study was approved by the Human Participants Ethics Committee of the Affiliated Brain Hospital of Nanjing Medical University. All subjects enrolled in this study provided written informed consent, see supplementary materials for details.

2.2. Clinical assessments

All participants underwent a standard clinical assessment that included detailed history collection, physical examination, and a battery of neuropsychological tests. The neuropsychological tests included the Mini-Mental State Examination (MMSE) (Tombaugh and McIntyre, 1992), the Montreal Cognitive Assessment (MoCA) (Horton et al., 2015), the CDR (Morris, 1993), the Auditory Verbal Learning Test (AVLT) (Vakil and Blachstein, 1993), the Clock-Drawing Test (CDT) (Mainland et al., 2014), the Boston Naming Test (BNT), the Verbal Fluency Test (VFT), the part A and B of the Trail Making Test (TMT-A/B), the Symbol Digit Modalities Test (SDMT), the Digit Span Test (DST) (Bowden et al., 2013), Hamilton anxiety scale (HAMA), Hamilton Depression scale (HAMD) (Bagby et al., 2004). These neuropsychological scales can evaluate general cognitive function, episodic memory, visuospatial function, language, executive function, attention and emotional state respectively. DLB and AD groups had CDR scores of 1 or 2 and MMSE scores of 14–26. All these scales were evaluated by experienced neuropsychologists.

2.3. Image acquisition

All MRI images were obtained from a 3.0 Tesla Verio Siemens scanner from the Department of Radiology of the Brain Hospital Affiliated to Nanjing Medical University. During the scanning, the heads of all participants were fixed and earplugs were used to reduce the effects of head movement and noise. Resting-state functional images were collected using the gradient-echo T2-weighted echo planar imaging sequence and an 8-channel head-coil when participants were specifically instructed to relax, remain still and awake, close their eyes, and not think about anything. The parameters were as follows: resolution = $3.4 \times 3.4 \times 4$ mm3, repetition time (TR) = 2000 ms, echo time (TE) = 30 ms, field of view (FOV) = 220 mm $\times$ 220 mm, flip angle (FA) = 90o, matrix = 64×64, slice number = 36, thickness = 4.0 mm, slice gap = 0 mm. The scan took about eight minutes. High-resolution T1 weighted images were acquired using 3D magnetization-prepared rapid gradient-echo sequence in a sagittal orientation for each subject. The parameters were: resolution = $1 \times 1 \times 1$ mm3, TR = 1900 ms, TE = 2.48 ms, inversion time (TI) = 900 ms, FOV = 256 mm $\times$ 256 mm, FA = 9°, matrix = 256×256, slice number = 176, thickness = 1.0 mm, slice gap = 0.5 mm. The scan took about four minutes.

2.4. Data processing

All preprocessing steps were performed by MATLAB 2014a and Data Processing & Analysis for Resting-State Brain Imaging (DPABI Version 4.3 http://rfmri.org/dpabi). The details regarding image preprocessing are consistent with previous studies (Ma et al., 2019). Specifically, the first 10 volumes were discarded to reduce the instability of the MRI signal. Corrections were performed for the slice timing and head motion. Participants with cumulative head motion > 3.0° or 3 mm were excluded (O'Callaghan et al., 2021). Then, these images were spatially normalized to standard Montreal Neurological Institute (MNI) space (3 $\times$ 3 $\times$ 3 mm3) using Diffeomorphic Anatomical Registration Through Exponentiated Lie algebra (DARTEL) and segmented into white matter, grey matter and cerebrospinal fluid. The white matter signal, cerebrospinal fluid signal and 24 motion parameters were regressed as nuisance covariate. Next, data were smoothed with 6 mm full-width half-maximum kernel (Schumacher et al., 2019; Schumacher et al., 2021) and detrended the linear and quadratic trends to reduce spatial noise. Finally, 0.01 ~ 0.08 Hz band-pass filter was used to reduce the influence of high-frequency physiological noise and low-frequency drift (Chen et al., 2016).

Rigorous quality assurance measures have been taken to reduce the impact of head movement on RS-fMRI results. First, in the process of data processing, we used the Friston 24-parameter model (Friston et al., 1996) to regress out head motion effects from the realigned data, which is based on the recent report that the high-order model shows an advantage in removing the head motion effect (Satterthwaite et al., 2013). Participants with cumulative head motion > 3.0°or 3 mm were excluded. Then, the visual examination steps in DPARSF were used to exclude subjects with severe head motion in the T1 image, subjects with extremely poor coverage in the functional image coverage and subjects with bad registration. At the same time, subjects with overlap with the group mask (voxels present at least 90% of the participants) <2*SD under the group mean overlap (threshold: 92%) and subjects with motion Mean FD Jenkinson>0.2 were excluded (Yan et al., 2013).

2.5. Regions of interest (ROIs) definition and network construction

In this study, 264 spherical ROIs with a radius of 5 mm were defined according to the coordinates defined by Power et al (Power et al., 2011). Then the mean time courses of each ROI was extracted. These ROIs cover 13 brain networks, which are default mode network (DMN), the frontoparietal network (FPN), sensorimotor network (SMN), ventral attention network (VAN), dorsal attention network (DAN), cingulo-opercular network (CON), auditory network (AUD), Visual network (VIS), memory retrieval (MEM), salience network (SN), subcortical network (SUB), cerebellum network (CN) and uncertain network. Considering that the function of the "uncertain" network is not clear, we mainly focus on the other 12 brain networks composed of 236 ROIs. Pearson's correlation coefficients were calculated by GRETNA software (http://www.nitrc.org/projects/gtetna/) between the mean time series of each pair of ROIs. As a result, we obtained a 236 $\times$ 236 symmetric connectivity matrix with Pearson's correlation coefficients as the weights. Then, Fisher's r-to-z transformation was performed for each correlation matrix to improve normality. Moreover, due to the unclear biological explanation of negative correlation (Chai et al., 2012; Murphy et al., 2009), we only focused on the difference of positive correlation matrix and set the diagonal value to zero. Finally, individual correlation matrices were threshold by a wide range of predefined sparsity (0.05–0.50, step = 0.05) based on the criteria proposed by previous studies (Lei et al., 2015; Zhang et al., 2011). The results of 15% sparsity (Wang et al., 2016) were reported in the main body, and other sparsity results were listed in the supplementary materials to ensure the stability of the results.

2.6. Rich club organization

2.6.1. Rich club coefficient

The assessment of rich club organization for each group was based on the group-averaged weighted network. For a given weighted network (matrix), first of all, the weights of each edge in the network are sorted from large to small. Secondly, for each degree k, the nodes with degree ≤ k are removed from the network, that is, nodes with degree value > k are selected to form a subnetwork. Then, the number of connected edges E > k and the sum of weights w > k are calculated. The weighted rich club coefficient Φ^w (k) was measured as the ratio between the sum of weights w > k of all connected edges in the subnetwork and the sum of the top E > k weights after sorting (van den Heuvel and Sporns, 2011). The Φ^w (k) is typically normalized (ϕ^w_{norm} (k)) by a set of "equivalent" random networks. A thousand random networks with equal size and degree distribution were created, and the average rich club coefficient Φ^w_{random} was calculated at each k level. The Φ^w_{norm} (k) was computed as the ratio between Φ^w (k) and Φ^w_{random}(k). A network is considered to have rich club organization if ϕ^w_{norm}(k) exceeds 1 in a continuous range of k (van den Heuvel and Sporns, 2011; Rubinov and Sporns, 2010). See the supplementary materials for the algorithm description of rich club coefficient and its normalized variant.

2.6.2. Hubs identification and connections classification

First, we calculate the degree of each node of each subject. The degree of an individual node is equal to the number of links connected to that node. The larger the degree of a node is, the more connections it has, and the more important the node is in the network. Then, as the previous studies did, rich club nodes of each group were defined as the top 18% of average node degree ranked nodes across all the participants in each group (Yan et al., 2018; Cao et al., 2020). The remaining brain nodes were defined as non-rich club nodes. Finally, according to the classification of rich club and non-rich club nodes, functional network connections were divided into three types of edges (van den Heuvel and Sporns, 2011): rich club connections, describing the connections between two rich club nodes, feeder connections, describing the connections between rich club nodes and non-rich club nodes, and local connections, describing the connections between two non-rich club nodes. We define the sum of all weights for each connection type as connectivity strength, which is a summary measure of connectivity (Yan et al., 2018).

To explore the restructuring characteristics of the rich club organization in each group, we further evaluated the distribution of the rich club nodes in spatial location and different functional networks. In addition, we further examined the inter-group differences based on whole-brain node degree values.

2.7. Statistical analysis

All statistical analyses were performed using Social Science Statistical Software Package (SPSS) version 20.0 (http://www.spss.com/). We used analysis of variance (ANOVA) to test for group differences in age and education level. Analysis of covariance (ANCOVA) were used to compare the differences of mean framewise displacement (FD) jenkinson, total intracranial volume (TIV), gray matter (GM) volume and GM/TIV ratio among the three groups with age and sex as covariables. Clinical assessments, normalized rich club coefficient, three types of connectivity strength and node degrees were compared among the three groups by ANCOVA with age and sex and GM volume as covariables. Post-hoc analyses were conducted using two-sample T-test ($p < 0.05$, Bonferroni correction). Chi-square test or Fisher's exact test were used to evaluate significant differences in gender distribution and node network distribution among the three groups. Finally, the relationship between connection strength and cognitive function in each group was evaluated by partial correlation analysis (corrected for age, sex and GM volume), with Bonferroni correction for multiple comparisons at $p < 0.05$.

2.8. Visualization

The visualization of 236 nodes on a brain surface was shown in supplementary Figure S1. All the brain surfaces were created using the BrainNet Viewer (http://nitrc.org/projects/bnv/).

3. Results

3.1. Demographic and clinical characteristics of subjects

Demographic and clinical information for patients and HC are summarized in Table 1. Subject groups were well matched for gender,

age and education ($p > 0.05$). No significant differences were found in disease duration between DLB and AD ($p > 0.05$). Mean FD Jenkinson had no significant difference among the three groups ($p > 0.05$). There was no significant difference in TIV among the three groups ($p > 0.05$). The GM volume and the GM/TIV ratio in DLB and AD groups were significantly lower than those in HC group ($p < 0.05$), but there was no significant difference between the two dementia groups ($p > 0.05$). The scores of general cognitive function (MMSE and MOCA), memory (AVLT delayed recall and REY delayed recall), language (VFT and BNT), visuospatial function (REY copy and CDT) and attention (DST and SDMT) were lower in DLB and AD groups compared with HC ($p < 0.05$). For executive function tests (TMT-A and TMT-B), the DLB and AD groups spent more time than HC group ($p < 0.05$). The AVLT recognition score of AD patients was significantly lower than that of HC ($p < 0.05$), while the score of DLB group was similar to that of HC group ($p > 0.05$). Patients with DLB and AD had more severe impairments in daily living and dementia assessment, as indicated by significantly higher ADL and CDR scores than the HC group ($p < 0.05$). In addition, patients with DLB were associated with more obvious anxiety and depression state, and their HAMA and HAMD scores were significantly higher than those of HC subjects ($p < 0.05$). For DLB and AD, there were no significant differences in general cognition, various cognitive domains and emotional state scores ($p > 0.05$), except that the ADL score of the DLB group was significantly higher than that of the AD group ($p < 0.05$).

3.2. Rich club organization

Fig. 1 shows the normalized rich club coefficient curves for AD (red), DLB (blue) and HC (green) based on group-averaged level. In our results, the rich club organization was found in the three groups. The normalized rich club curves show an increasing ϕ^w_{norm} (k) higher than 1 over a range of k for both patient groups and HC. In the whole-brain network,

Table 1
Demographic and clinical characteristics of subjects.

Characteristics	AD (n = 34)	DLB (n = 30)	HC (n = 33)	Test statistic	p
Gender (male/female)	14/20	17/13	15/18	χ2 = 1.611	0.447
Age (y)	65.88 ± 8.26	67.43 ± 5.32	64.94 ± 9.39	F = 0.790	0.457
Education level (y)	9.62 ± 4.81	9.07 ± 2.79	10.76 ± 3.11	F = 1.717	0.185
Disease duration (mo)	30.65 ± 16.92	25.30 ± 14.98	—	T = 1.341	0.185
Mean FD_Jenkinson (mm)	0.096 ± 0.050	0.120 ± 0.053	0.095 ± 0.501	F = 1.194	0.308
TIV (cm³)	1406.88 ± 161.52	1486.03 ± 133.54	1377.82 ± 128.96	F = 2.447	0.092
GM volume (cm³)	475.03 ± 44.18	493.57 ± 51.63	536.70 ± 46.86	F = 16.894	<0.001[ab]
GM/TIV (%)	33.93 ± 2.76	33.23 ± 1.99	39.05 ± 2.81	F = 49.281	<0.001[ab]
MMSE	16.12 ± 6.15	17.63 ± 6.09	28.03 ± 1.36	F = 35.277	<0.001[ab]
MoCA	10.25 ± 5.34	11.48 ± 6.02	27.09 ± 1.55	F = 93.844	<0.001[ab]
AVLT delayed recall	0.22 ± 0.68	0.50 ± 0.84	5.45 ± 2.17	F = 47.888	<0.001[ab]
AVLT recognition	13.82 ± 4.66	18.67 ± 2.50	21.39 ± 1.87	F = 16.164	<0.001[a]
REY delayed recall	1.19 ± 2.66	3.07 ± 3.25	17.19 ± 7.20	F = 45.034	<0.001[ab]
REY copy	16.96 ± 11.74	17.07 ± 12.70	34.76 ± 1.52	F = 22.754	<0.001[ab]
VFT	7.45 ± 3.25	8.17 ± 3.43	17.91 ± 5.15	F = 28.851	<0.001[ab]
BNT	14.83 ± 5.50	12.00 ± 7.21	24.97 ± 1.81	F = 31.798	<0.001[ab]
TMT-A	162.52 ± 50.07	171.60 ± 131.90	61.00 ± 16.72	F = 19.103	<0.001[ab]
TMT-B	311.43 ± 39.23	346.33 ± 39.17	139.30 ± 44.42	F = 61.045	<0.001[ab]
CDT	15.40 ± 9.61	16.17 ± 8.70	27.67 ± 2.26	F = 14.855	<0.001[ab]
DST	5.18 ± 2.65	7.00 ± 1.67	9.03 ± 1.81	F = 12.282	<0.001[ab]
SDMT	10.07 ± 10.24	18.00 ± 8.54	44.82 ± 10.44	F = 44.134	<0.001[ab]
ADL	29.24 ± 5.15	32.82 ± 11.87	20.55 ± 0.71	F = 19.972	<0.001[abc]
CDR	1.26 ± 0.60	1.20 ± 0.86	0.00 ± 0.00	F = 35.371	<0.001[ab]
HAMA	4.70 ± 2.81	5.50 ± 2.00	2.82 ± 1.74	F = 4.726	0.001[b]
HAMD	3.87 ± 3.13	5.38 ± 1.92	2.30 ± 1.63	F = 4.001	0.002[b]

Note: Numbers are expressed as mean ± SD.

Only 6 to 8 patients with DLB had the data of each cognitive domain assessment.

AD = Alzheimer's disease, DLB = Dementia with Lewy body, HC = healthy control, FD = framewise displacement, TIV = Total intracranial volume, GM = Gray matter, MMSE = Mini Mental State Examination, MoCA = Montreal Cognitive Assessment, AVLT = Auditory Verbal Learning Test, REY = Rey complex figure test, VFT = Verbal Fluency Test, BNT = Boston Naming Test, TMT = Trail Making Test, CDT = Clock-Drawing Test, DST = Digit Span Test, SDMT = Symbol Digit Modalities Test, ADL = Activity of Daily Living Scale, CDR = Clinical Dementia Rating, HAMA = Hamilton anxiety scale, HAMD = Hamilton Depression scale, y = years, mo = months.

[a] HC group and AD patients showed significant differences ($p < 0.05$).

[b] HC group and DLB patients showed significant differences ($p < 0.05$).

[c] DLB patients and AD patients showed significant differences ($p < 0.05$).

Fig. 1. Group-averaged normalized rich club coefficient curves for AD (red), DLB (blue) and HC (green). For both dementia groups and HC, the increasing ϕ^w_{norm} (k) was>1 over a range of k. There was no significant difference in the ϕ^w_{norm} (k) among three groups at any k level. The data depicted are from 15% network density. Results are similar for other thresholds (See Supplementary Figure S2). (For interpretation of the references to colour in this figure legend, the reader is referred to the web version of this article.)

there was no significant difference in the normalized rich club coefficient ϕ^w_{norm} (k) among the three groups at any k level. (ANCOVA; age, sex and GM volume as covariates; Bonferroni corrected) (Detailed data are shown in Table S1).

3.3. Spatial location of rich club nodes

The details of rich club nodes in the three different groups are shown in Fig. 2 and Table 2. Finally, we selected 43 nodes in each group (the top 18% of nodes in the average node degree of all participants in each group). As shown in Fig. 2 and Table 2, the distribution of rich club nodes in the three groups all involved frontal, parietal, temporal, occipital and cingulate gyrus. However, the location distribution of rich club nodes was different among the three groups. In HC group, rich club nodes were mostly evenly distributed among the right middle frontal gyrus, precentral gyrus, bilateral postcentral gyrus, supplementary motor area, inferior parietal lobule, superior temporal gyrus, middle temporal gyrus, cuneus, precuneus, occipital lobe and bilateral cingulate gyrus. Subcortical rich club node is the left thalamus. Although the rich club nodes in AD group were also mainly distributed in the frontal lobe, parietal lobe, temporal lobe, occipital lobe and cingulate gyrus, the number of rich club nodes involved in temporal lobe was significantly smaller. More interestingly, two rich club nodes appeared in the cerebellum, accompanied by a subcortical rich club node in the right caudate

nucleus. Compared with AD group, there seemed to be more obvious distribution difference between DLB and HC group, mainly manifested in the obvious increase in the number of rich club nodes in frontal lobe and parietal lobe of DLB patients. The number of rich club nodes in temporal lobe was between AD and HC, and there was no rich club node in the subcortical basal ganglia.

3.4. Distribution of rich club nodes in different functional networks

As shown in Fig. 3 and Table 3, the percentages of rich club nodes in different functional networks are different among the three groups. The rich club nodes distribution of AD group involved 10 networks, mainly including DMN (30.23%), VIS (18.60%), SN (11.63%), and others were uniformly distributed in the SMN (6.98%), CON (6.98%), MEM (6.98%), FPN (4.65%), SUB (2.33%), DAN (6.98%), CN (4.65%). There are no rich club nodes in AUD and VAN. In DLB group, rich club nodes are involved in 8 networks, mainly distributed in DMN (41.86%) and FPN (23.26%), and the rest networks include VIS (9.30%), MEM (9.30%), SN (9.30%), VAN (2.33%), DAN (2.33%), and SMN (2.33%). The CON, AUD, SUB, CN have no rich club nodes. The proportion of nodes involved in SMN was significantly lower than that in HC group ($p <$ 0.05), while the proportion of nodes involved in FPN was significantly higher than that in AD and HC groups ($p < 0.05$) (Table 3). All rich club nodes in HC group were mainly located in the DMN (20.93%), SMN (18.60%), VIS (18.60%) and SN (13.95%), and others were uniformly distributed in the CON (6.98%), AUD (2.33%), MEM (4.65%), FPN (4.65%), SUB (2.33%), VAN (2.33%), DAN (4.65%), involving 11 brain networks. None of the rich club nodes were observed in the CN network.

3.5. Strength of rich club, feeder and local connections

Statistical analysis showed that strength of rich club connection in DLB and AD group was significantly higher than that in HC group (DLB, $p < 0.01$; AD, $p < 0.01$, Bonferroni correction). However, there was no difference in feeder and local connections between patients and HC. In addition, no differences were found in all three types of connections between DLB and AD group (Fig. 4 and Table 4). Fig. 5 shows a schematic diagram of two types of nodes and three types of connections.

3.6. Differences in node degree among the three groups

To determine exactly which regions were altered, we analyzed the differences between groups for all node degrees in the whole brain quantitatively (Fig. 6, Table 5).
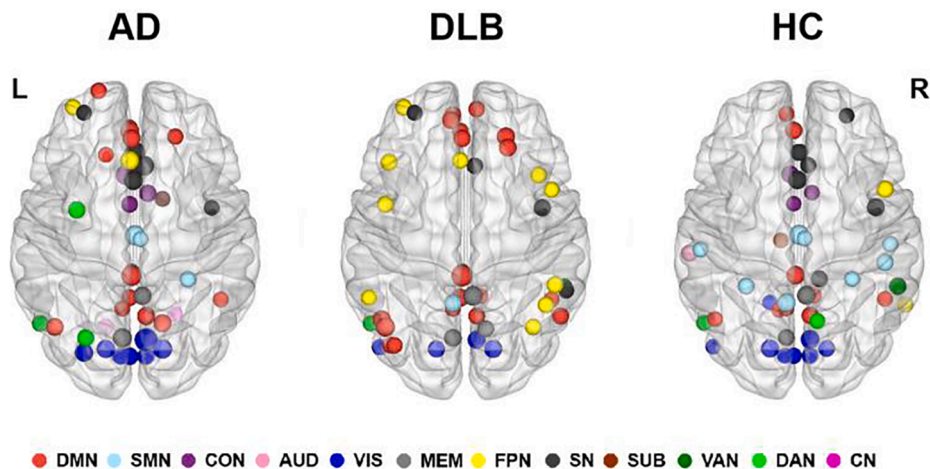
Fig. 2. Distribution of rich club nodes in the whole brain network of AD (left), DLB (middle) and HC (right). The different colors represent different brain functional networks. The size of nodes reflects the group average degree of each node. L = Left, R = Right.

Table 2
Location and network information of rich club nodes in each group.

Number	MNI x	y	z	Brain Region	Network
AD					
1	−16	29	53	Frontal_Sup_L	DMN
2	−20	64	19	Frontal_Sup_L	DMN
3	22	39	39	Frontal_Sup_R	DMN
4	−2	38	36	Frontal_Sup_Medial_L	DMN
5	−3	26	44	Frontal_Sup_Medial_L	FPN
6	−34	55	4	Frontal_Mid_L	FPN
7	−28	52	21	Frontal_Mid_L	SN
8	−32	−1	54	Frontal_Mid_L	DAN
9	−3	44	−9	Frontal_Med_Orb_L	DMN
10	−3	2	53	Supp_Motor_Area_L	CON
11	7	8	51	Supp_Motor_Area_R	CON
12	3	−17	58	Supp_Motor_Area_R	SMN
13	42	0	47	Precentral_R	SN
14	29	−39	59	Postcentral_R	SMN
15	−44	−65	35	Angular_L	DMN
16	47	−50	29	Angular_R	DMN
17	−7	−71	42	Precuneus_L	MEM
18	−7	−55	27	Precuneus_L	DMN
19	15	−63	26	Precuneus_R	DMN
20	4	−48	51	Precuneus_R	MEM
21	6	−59	35	Precuneus_R	DMN
22	−3	−81	21	Cuneus_L	VIS
23	−16	−77	34	Cuneus_L	VIS
24	6	−72	24	Cuneus_R	VIS
25	15	−77	31	Cuneus_R	VIS
26	−8	−81	7	Calcarine_L	VIS
27	6	−81	6	Calcarine_R	VIS
28	8	−72	11	Calcarine_R	VIS
29	−28	−79	19	Occipital_Mid_L	VIS
30	−27	−71	37	Occipital_Sup_L	DAN
31	−52	−63	5	Temporal_Inf_L	DAN
32	−3	42	16	Cingulum_Ant_L	DMN
33	0	30	27	Cingulum_Ant_L	SN
34	−2	−37	44	Cingulum_Mid_L	DMN
35	−5	18	34	Cingulum_Mid_L	CON
36	0	−15	47	Cingulum_Mid_L	SMN
37	−1	15	44	Cingulum_Mid_L	SN
38	5	23	37	Cingulum_Mid_R	SN
39	−2	−35	31	Cingulum_Post_L	MEM
40	−3	−49	13	Cingulate Gyrus_L	DMN
41	15	5	7	Caudate_R	SUB
42	−16	−65	−20	Cerebelum_6_L	CN
43	22	−58	−23	Cerebelum_6_R	CN
DLB					
1	−2	38	36	Frontal_Sup_Medial_L	DMN
2	−8	48	23	Frontal_Sup_Medial_L	DMN
3	−3	26	44	Frontal_Sup_Medial_L	FPN
4	6	54	16	Frontal_Sup_Medial_R	DMN
5	22	39	39	Frontal_Sup_R	DMN
6	23	33	48	Frontal_Sup_R	DMN
7	40	18	40	Frontal_Mid_R	FPN
8	−34	55	4	Frontal_Mid_L	FPN
9	−28	52	21	Frontal_Mid_L	SN
10	−39	−75	44	Parietal_Inf_L	DMN
11	−53	−49	43	Parietal_Inf_L	FPN
12	44	−53	47	Parietal_Inf_R	FPN
13	−42	25	30	Frontal_Inf_Tri_L	FPN
14	49	−42	45	SupraMarginal_R	FPN
15	55	−45	37	SupraMarginal_R	SN
16	37	−65	40	Angular_R	FPN
17	−44	−65	35	Angular_L	DMN
18	47	−50	29	Angular_R	DMN
19	52	−59	36	Angular_R	DMN
20	−44	2	46	Precentral_L	FPN
21	−7	−71	42	Precuneus_L	MEM
22	−7	−52	61	Precuneus_L	SMN
23	−7	−55	27	Precuneus_L	DMN
24	42	0	47	Precentral_R	SN
25	11	−66	42	Precuneus_R	MEM
26	4	−48	51	Precuneus_R	MEM
27	47	10	33	Precentral_R	FPN
28	6	−59	35	Precuneus_R	DMN
29	−16	−77	34	Cuneus_L	VIS
30	15	−77	31	Cuneus_R	VIS
31	6	−72	24	Cuneus_R	VIS
32	−47	−76	−10	Occipital_Inf_L	VIS
33	−41	−75	26	Occipital_Mid_L	DMN
34	54	−43	22	Temporal_Sup_R	VAN
35	−52	−63	5	Temporal_Mid_L	DAN
36	−46	−61	21	Temporal_Mid_L	DMN
37	−3	−49	13	Cingulate Gyrus_L	DMN
38	−2	−37	44	Cingulate Gyrus_L	DMN
39	−7	51	−1	Cingulum_Ant_L	DMN
40	−3	42	16	Cingulum_Ant_L	DMN
41	5	23	37	Cingulum_Mid_R	SN
42	−2	−35	31	Cingulum_Post_L	MEM
43	8	−48	31	Cingulum_Post_R	DMN
HC					
1	26	50	27	Frontal_Mid_R	SN
2	−3	2	53	Supp_Motor_Area_L	CON
3	7	8	51	Supp_Motor_Area_R	CON
4	3	−17	58	Supp_Motor_Area_R	SMN
5	47	10	33	Precentral_R	FPN
6	42	0	47	Precentral_R	SN
7	−29	−43	61	Postcentral_L	SMN
8	29	−39	59	Postcentral_R	SMN
9	50	−20	42	Postcentral_R	SMN
10	47	−30	49	Parietal_Inf_R	SMN
11	−54	−23	43	SupraMarginal_L	SMN
12	47	−50	29	Angular_R	DMN
13	−7	−71	42	Precuneus_L	MEM
14	−7	−55	27	Precuneus_L	DMN
15	−11	−56	16	Precuneus_L	DMN
16	−7	−52	61	Precuneus_L	SMN
17	4	−48	51	Precuneus_R	MEM
18	6	−59	35	Precuneus_R	DMN
19	10	−62	61	Precuneus_R	DAN
20	−16	−77	34	Cuneus_L	VIS
21	−3	−81	21	Cuneus_L	VIS
22	15	−77	31	Cuneus_R	VIS
23	6	−72	24	Cuneus_R	VIS
24	−8	−81	7	Calcarine_L	VIS
25	6	−81	6	Calcarine_R	VIS
26	−47	−76	−10	Occipital_Inf_L	VIS
27	−16	−52	−1	Lingual_L	VIS
28	−60	−25	14	Temporal_Sup_L	AUD
29	54	−43	22	Temporal_Sup_R	VAN
30	−46	−61	21	Temporal_Mid_L	DMN
31	−52	−63	5	Temporal_Mid_L	DAN
32	58	−53	−14	Temporal_Inf_R	FPN
33	−7	51	−1	Cingulum_Ant_L	DMN
34	−3	42	16	Cingulum_Ant_L	DMN
35	0	30	27	Cingulum_Ant_L	SN
36	0	−15	47	Cingulum_Mid_L	SMN
37	−5	18	34	Cingulum_Mid_L	CON
38	−2	−37	44	Cingulum_Mid_L	DMN
39	−1	15	44	Cingulum_Mid_L	SN
40	5	23	37	Cingulum_Mid_R	SN
41	11	−39	50	Cingulum_Mid_R	SN
42	8	−48	31	Cingulum_Post_R	DMN
43	−10	−18	7	Thalamus_L	SUB

Note: DMN: the default mode network, SMN: sensory/somatomotor network, CON: cingulo-opercular task control network, AUD: auditory network, VIS: visual network, MEM: memory retrieval network, FPN: fronto-parietal task control network, SN: salience network, SUB: subcortical network, VAN: ventral attention network, DAN: dorsal attention network, CN: cerebellum network. AD = Alzheimer's disease, DLB = Dementia with Lewy body, HC = healthy control.

3.6.1. AD versus HC

Nodal degree increased in AD, relative to controls at 8 ROIs. These affected brain regions were predominantly located in the frontal lobe (left superior frontal gyrus, left medial superior frontal gyrus) and cerebellum (right cerebelum_crus1, bilateral cerebelum_6, and vermis_6), as well as the right cuneus and left middle occipital gyrus in the posterior part of the brain, with an overall front-back distribution. Among these
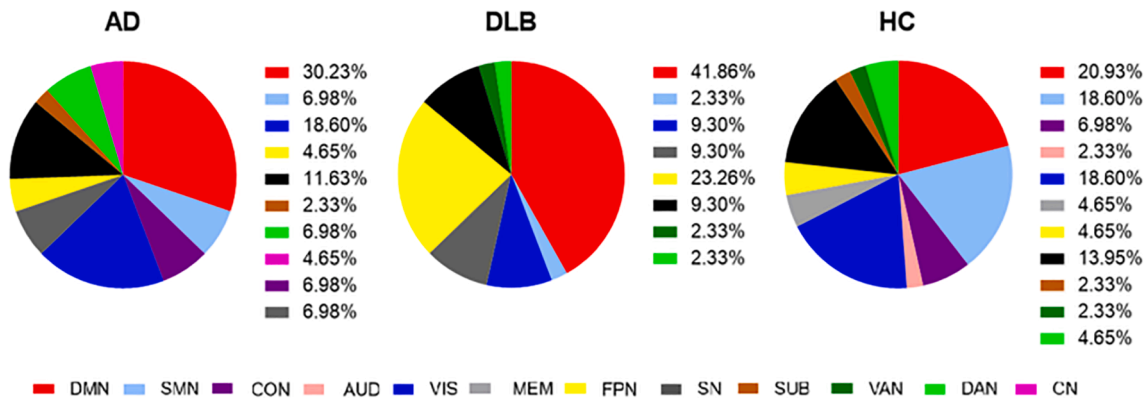
Fig. 3. Percentage of rich club nodes in the different functional networks of AD (left), DLB (middle) and HC (right). The different colors represent different brain functional networks.

Table 3
Network distribution of rich club nodes in each group.

Network	AD	DLB	HC	Test statistic	p
DMN	13	18	9	4.421[A]	0.110
SMN	3	1	8	6.503[B]	0.041[b]
CON	3	0	3	3.372[B]	0.245
AUD	0	0	1	—	—
VIS	8	4	8	1.894[A]	0.388
MEM	3	4	2	0.773[B]	0.908
FPN	2	10	2	8.830[B]	0.013[bc]
SN	5	4	6	0.453[A]	0.797
SUB	1	0	1	—	—
VAN	0	1	1	—	—
DAN	3	1	2	1.08	0.871
CN	2	0	0	—	—

Note: The data depicted are from 15% network density.
DMN: the default mode network, SMN: sensory/somatomotor network, CON: cingulo-opercular task control network, AUD: auditory network, VIS: visual network, MEM: memory retrieval network, FPN: fronto-parietal task control network, SN: salience network, SUB: subcortical network, VAN: ventral attention network, DAN: dorsal attention network, CN: cerebellum network. AD = Alzheimer's disease, DLB = Dementia with Lewy body, HC = healthy control.
[A] Pearson Chi-Square.
[B] Fisher's Exact Test.
[b] DLB patients and HC group showed significant differences ($p < 0.05$).
[c] DLB patients and AD patients showed significant differences ($p < 0.05$).

affected nodes, three belong to DMN and three belong to CN. In addition, VIS have two nodes (Fig. 6A, Table 5).

The nodal degree was significantly lower in AD patients, relative to HC in 11 regions. The most significant deficits were found in and around the temporal lobe (bilateral middle temporal gyrus, left heschl's gyrus, right superior temporal gyrus, left fusiform gyrus and lingual gyrus) and

frontal and parietal junction (right precentral gyrus and left rolandic operculum), presenting a left–right distribution. Among the affected nodes, 4 belong to DMN, 3 belong to AUD, and 2 belong to SUB network. In addition, VIS and DAN each have one affected node (Fig. 6B, Table 5).

3.6.2. DLB versus HC

Compared with the HC group, the DLB patients had 7 significantly increased brain regions, of which 4 belonged to FPN, distributed in bilateral inferior parietal gyrus, bilateral middle frontal gyrus, respectively, and 3 belonged to DMN, located in left angular gyrus and left inferior parietal gyrus and right superior frontal gyrus (Fig. 6C, Table 5).

Compared with HC group, there were only three regions with significant reduction in nodal degree in DLB patients, which were right supplementary motor area and right postcentral gyrus belonging to SMN, and left superior marginal gyrus belonging to AUD (Fig. 6D, Table 5).

Table 4
Strength of rich club, feeder and local connections in each group.

Connection type	AD	DLB	HC	F	p
Rich Club	276.94 ± 87.48	261.90 ± 105.43	215.27 ± 67.74	4.168	0.018[ab]
Feeder	1059.68 ± 189.55	991.30 ± 203.63	1022.70 ± 144.94	1.345	0.266
Local	5879.29 ± 467.16	6033.70 ± 513.53	6130.70 ± 727.96	0.501	0.608

Note: Numbers are expressed as mean ± SD.
AD = Alzheimer's disease, DLB = Dementia with Lewy body, HC = healthy control.
[a] HC group and AD patients showed significant differences ($p < 0.05$).
[b] HC group and DLB patients showed significant differences ($p < 0.05$).
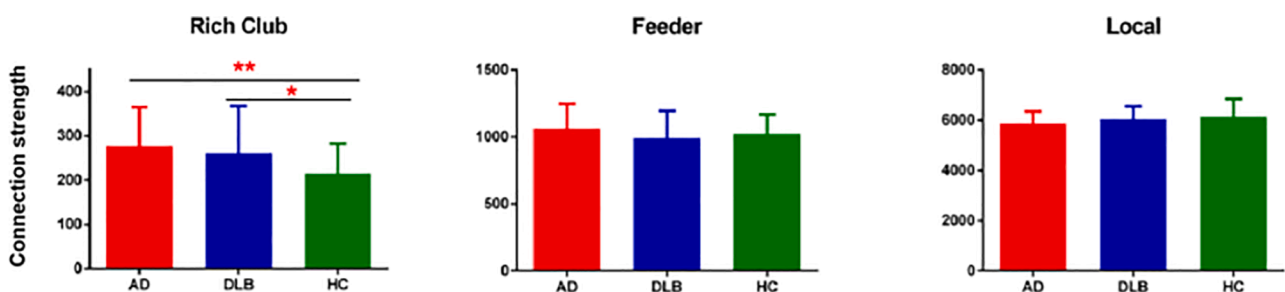
Fig. 4. Strength of rich club, feeder and local connections. Bar graphs showed the mean strength of rich club, feeder and local connections for each group. Error bars expressed standard deviation of measures over the group. The asterisks indicated the statistically significant difference between groups (**$p < 0.01$, * $p < 0.05$). For rich club connection strength, there were significant increases in the AD ($p = 0.005$) and DLB ($p = 0.038$) groups relative to the HC group. However, there was no significant difference in feeder (F = 1.152, $p = 0.32$) and local (F = 1.593, $p = 0.209$) connection strength among three groups (ANCOVAs: age and sex as covariates).
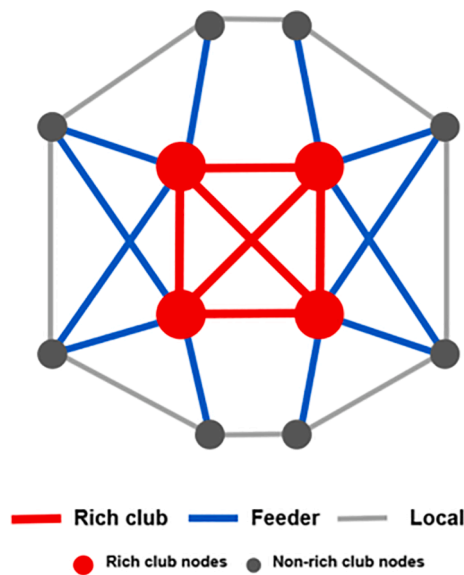
Fig. 5. The different kinds of connections in functional networks. Edges across individual brain networks were divided into rich club (red), feeder (blue), and local connections (gray). (For interpretation of the references to colour in this figure legend, the reader is referred to the web version of this article.)

3.6.3. AD versus DLB

The nodal degree of 10 regions in AD group was significantly increased relative to DLB group. The affected nodes were mainly distributed in left anterior cingulate gyrus, left middle cingulate gyrus, right precentral gyrus, supplementary motor area, precuneus, cuneus, orbital part of inferior frontal gyrus and left calcarine fissure. Two of the affected nodes were part of the SMN and three of the affected nodes were part of the VIS. (Fig. 6E, Table 5).

AD patients had a lower nodal degree, relative to DLB in 8 regions of the brain mostly distributed in temporal lobe and its surrounding (left middle temporal gyrus, bilateral fusiform gyrus and left rolandic operculum) and frontal-parietal lobe (right superior marginal gyrus, left inferior parietal gyrus and right precentral gyrus) (Fig. 6F, Table 5). Three of the affected nodes were in DMN and 3 were FPN.

3.7. The relationship between connection strength and clinical characteristics

In exploratory analyses, we correlated three types of connection strength with cognitive function assessments in DLB and AD group, with age, sex and GM volume as covariates (Table 6). In patients with DLB, connection strength showed significant correlation with certain cognitive assessments. In patients with AD, however, there was no correlation between connection strength and any clinical features. For DLB patients, there was a negative linear correlation between the BNT score and local connection strength ($r = -0.953$, $p = 0.047$, Fig. 7A). In addition, DST score of DLB patients was positively correlated with Feeder FC strength ($r = 0.932$, $p = 0.021$, Fig. 7B), and negatively correlated with local connection strength ($r = -0.939$, $p = 0.018$, Fig. 7C). No significant correlation was observed between connection strength and other clinical variables in DLB.

4. Discussion

In this study, we constructed the brain functional networks of AD, DLB and HC, and analyzed the organizational level and structural characteristics of Rich Club in each group. The results showed that although the phenomenon of Rich Club organization existed in all three groups, the spatial location and network distribution of rich club nodes
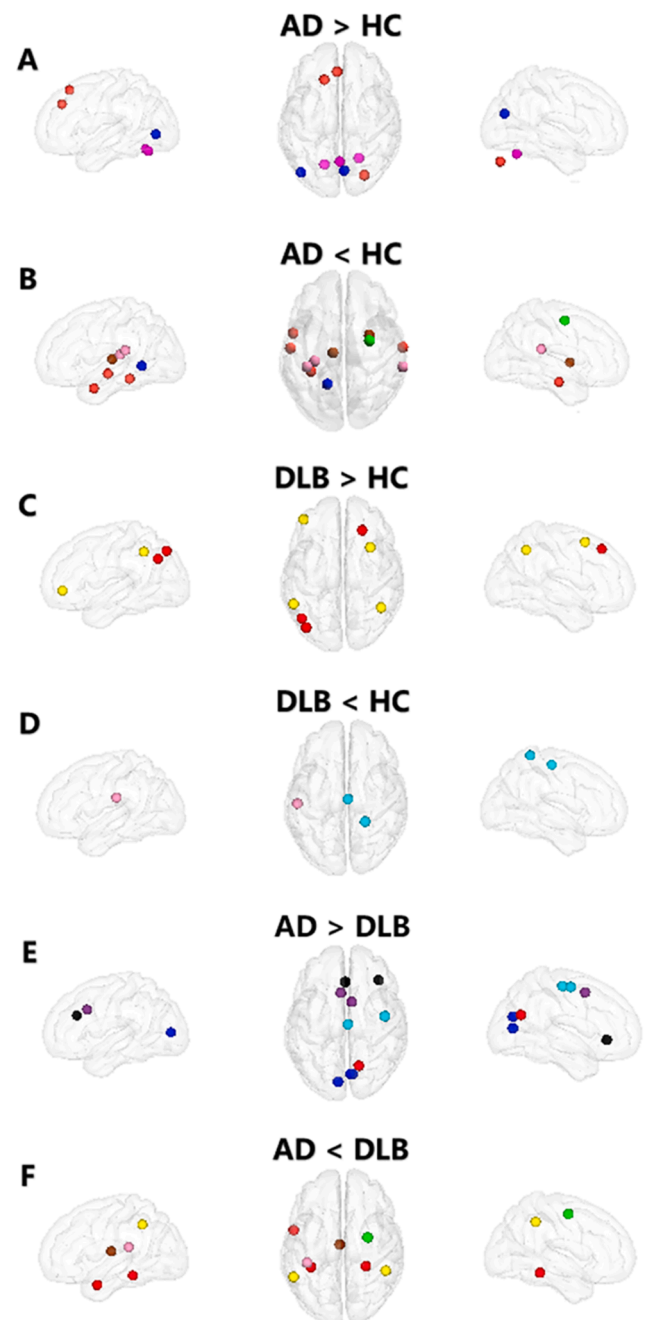
Fig. 6. Differences in node degree among the three groups. Rendering plots of the brain regions that showed significantly different node degree among the three groups. Different colors represent different brain functional networks. (A) Increases in nodal degree in AD, versus controls, at 8 distinct nodes predominantly located in the frontal lobe and cerebellum, and the altered nodes were mainly involved in DMN and CN. (B) Decreases in nodal degree in AD, versus controls, at 11 distinct nodes mainly distributed among DMN, AUD and attention internets; note that most significantly altered nodes were in and around the temporal lobe, as well as frontal and parietal junction. (C) Increases in nodal degree in DLB, versus controls, across 7 nodes with largest proportion of these nodes located in the FPN. (D) Decreases in nodal degree in DLB, versus controls, across 3 nodes, which were 2 nodes in SMN and 1 node in AUD. (E) Increases in nodal degree in AD, versus DLB, at 10 nodes with an overall front-back distribution. (F) Decreases in nodal degree in AD, versus DLB, at 18 nodes with a left–right distribution.

Table 5
Information of nodes with inter-group differences in node degree.

Number	MNI X	Y	Z	Brain Region	Network	Degree of Group 1	Degree of Group 2	p
AD < HC						AD	HC	
1	−56	−13	−10	Temporal_Mid_L	DMN	21.103 ± 18.937	32.067 ± 20.844	0.0297
2	−34	−38	−16	Fusiform_L	DMN	13.000 ± 10.573	22.233 ± 17.934	0.0327
3	−53	3	−27	Temporal_Mid_L	DMN	17.241 ± 11.372	28.633 ± 21.224	0.0163
4	65	−12	−19	Temporal_Mid_R	DMN	28.379 ± 17.030	35.833 ± 24.080	0.036
5	65	−33	20	Temporal_Sup_R	AUD	21.310 ± 17.599	32.900 ± 21.083	0.0250
6	−38	−33	17	Rolandic_Oper_L	AUD	13.690 ± 13.465	29.167 ± 19.631	0.0012
7	−30	−27	12	Heschl_L	AUD	18.138 ± 19.220	28.833 ± 21.091	0.0327
8	−16	−52	−1	Lingual_L	VIS	29.034 ± 20.876	42.933 ± 18.986	0.0103
9	29	1	4	Putamen_R	SUB	25.621 ± 16.269	38.467 ± 20.961	0.0086
10	−10	18	7	Thalamus_L	SUB	32.103 ± 22.800	42.700 ± 24.111	0.038
11	29	−5	54	Precentral_R	DAN	27.517 ± 12.336	42.067 ± 25.100	0.0064
AD > HC						AD	HC	
1	−16	29	53	Frontal_Sup_L	DMN	43.690 ± 21.912	32.367 ± 21.877	0.0442
2	−2	38	36	Frontal_Sup_Medial_L	DMN	50.138 ± 22.668	38.500 ± 17.344	0.0497
3	28	−77	−32	Cerebelum_Crus1_R	DMN	39.724 ± 24.104	26.933 ± 18.504	0.0301
4	6	−72	24	Cuneus_R	VIS	62.517 ± 21.738	51.533 ± 20.812	0.0366
5	−42	−74	0	Occipital_Mid_L	VIS	40.621 ± 19.177	33.500 ± 19.396	0.031
6	−16	−65	−20	Cerebelum_6_L	CN	45.724 ± 24.865	25.767 ± 19.851	0.0011
7	22	−58	−23	Cerebelum_6_R	CN	43.310 ± 24.074	25.200 ± 22.397	0.0039
8	1	−62	−18	Vermis_6	CN	38.069 ± 20.064	23.567 ± 19.695	0.0070
DLB < HC						DLB	HC	
1	3	−17	58	Supp_Motor_Area_R	SMN	29.500 ± 14.990	43.300 ± 24.315	0.016
2	22	−42	69	Postcentral_R	SMN	25.267 ± 16.918	38.364 ± 22.669	0.0112
3	−53	−22	23	SupraMarginal_L	AUD	27.167 ± 17.167	37.545 ± 19.221	0.0339
DLB > HC						DLB	HC	
1	−44	−65	35	Angular_L	DMN	51.133 ± 21.793	40.121 ± 19.939	0.0344
2	−39	−75	44	Parietal_Inf_L	DMN	43.600 ± 21.550	31.273 ± 19.585	0.0160
3	23	33	48	Frontal_Sup_R	DMN	49.050 ± 24.979	37.033 ± 18.940	0.031
4	−53	−49	43	Parietal_Inf_L	FPN	44.533 ± 21.245	31.697 ± 17.657	0.0110
5	44	−53	47	Parietal_Inf_R	FPN	46.167 ± 22.626	35.758 ± 18.805	0.0374
6	−42	45	−2	Frontal_Mid_Orb_L	FPN	43.800 ± 20.734	28.727 ± 16.525	0.0037
7	32	14	56	Frontal_Mid_R	FPN	36.000 ± 26.523	25.533 ± 16.600	0.044
AD < DLB						AD	DLB	
1	27	−37	−13	Fusiform_R	DMN	15.483 ± 16.030	27.500 ± 22.016	0.0156
2	−34	−38	−16	Fusiform_L	DMN	13.000 ± 10.573	28.100 ± 20.183	0.0021
3	−53	3	−27	Temporal_Mid_L	DMN	17.241 ± 11.372	31.350 ± 19.720	0.0079
4	−38	−33	17	Rolandic_Oper_L	AUD	13.690 ± 13.465	25.650 ± 19.752	0.0224
5	−53	−49	43	Parietal_Inf_L	FPN	32.345 ± 16.655	43.450 ± 21.172	0.0358
6	49	−42	45	SupraMarginal_R	FPN	35.552 ± 19.613	47.500 ± 21.717	0.0451
7	−2	−13	12	Thalamus_L	SUB	14.655 ± 15.363	24.800 ± 19.509	0.0471
8	29	−5	54	Precentral_R	DAN	27.517 ± 12.336	41.600 ± 20.009	0.0173
AD > DLB						AD	DLB	
1	15	−63	26	Precuneus_R	DMN	50.138 ± 23.570	34.350 ± 15.742	0.0064
2	44	−8	57	Precentral_R	SMN	40.655 ± 25.773	24.850 ± 14.751	0.0135
3	3	−17	58	Supp_Motor_Area_R	SMN	43.690 ± 28.311	29.500 ± 14.989	0.0456
4	−5	18	34	Cingulum_Mid_L	CON	55.897 ± 23.437	38.400 ± 19.346	0.0069
5	7	8	51	Supp_Motor_Area_R	CON	47.586 ± 18.675	37.950 ± 21.539	0.008
6	−8	−81	7	Calcarine_L	VIS	46.862 ± 19.026	35.700 ± 19.013	0.0336
7	6	−72	24	Cuneus_R	VIS	62.517 ± 21.738	49.800 ± 14.634	0.0303
8	8	−72	11	Calcarine_R	VIS	47.345 ± 23.990	38.100 ± 23.389	0.037
9	37	32	−2	Frontal_Inf_Orb_R	SN	30.207 ± 17.775	19.050 ± 14.609	0.0274
10	0	30	27	Cingulum_Ant_L	SN	58.276 ± 21.870	42.550 ± 19.381	0.0124

Note: DMN: the default mode network, SMN: sensory/somatomotor network, CON: cingulo-opercular task control network, AUD: auditory network, VIS: visual network, MEM: memory retrieval network, FPN: fronto-parietal task control network, SN: salience network, SUB: subcortical network, VAN: ventral attention network, DAN: dorsal attention network, CN: cerebellum network. AD = Alzheimer's disease, DLB = Dementia with Lewy body, HC = healthy control.

in each group were different. When comparing all nodes in the whole brain, both AD and DLB groups showed a combination of decreased node degree damage related to pathologic basis or clinical symptoms of the disease and increased node degree regulated by compensatory mechanism. In addition, we found a significant increase in Rich Club connection strength in both DLB and AD groups, and for DLB, the connectivity strength correlated with cognitive assessment. In summary, these findings suggest that the normal structure of the Rich Club organization in DLB and AD patients is destroyed, accompanied by different characteristics of reorganization. This can provide a new perspective for a comprehensive understanding of the pathophysiological mechanisms of DLB and AD, and thus provide a basis for the formulation of disease-specific diagnosis and treatment.

4.1. Rich club organization in DLB, AD and HC groups

Rich club organization is a common attribute of complex networks, which has been observed in both human structural and functional networks. The rich club phenomenon is found not only in the brains of adults, but also in the brains of newborns (Ball et al., 2014), and is supposed to be the communication center of the entire brain network (van den Heuvel and Sporns, 2011). Low-k regions include low-degree nodes that form local clusters and isolated connectome populations and provide a communication relay that aids in the global integration of information in the brain (de Reus and van den Heuvel, 2013; Sporns, 2011). The high k-value regions only retain the most closely connected nodes in the connectome (van den Heuvel et al., 2009). Communication

Table 6

Correlation analysis between connection strength and clinical characteristics.

COV:Sex & Age		AD Rich Club	Feeder	Local	DLB Rich Club	Feeder	Local
Disease duration (mo)	r	−0.014	0.122	−0.101	−0.212	−0.167	0.190
	p	0.940	0.514	0.589	0.288	0.404	0.341
MMSE	r	0.009	−0.014	−0.002	0.284	0.183	−0.215
	p	0.964	0.941	0.991	0.160	0.370	0.292
MoCA	r	−0.101	−0.108	0.097	0.349	0.271	−0.292
	p	0.603	0.577	0.615	0.080	0.181	0.148
AVLT delayed recall	r	−0.221	−0.164	0.156	0.580	0.058	−0.121
	p	0.300	0.444	0.466	0.4420	0.942	0.879
AVLT recognition	r	−0.028	−0.072	0.059	−0.762	−0.522	0.564
	p	0.898	0.740	0.784	0.238	0.478	0.436
REY delayed recall	r	−0.167	−0.154	0.158	0.903	0.775	−0.835
	p	0.436	0.473	0.462	0.097	0.225	0.165
REY imitation	r	0.090	0.056	−0.076	0.799	0.437	−0.546
	p	0.676	0.794	0.723	0.201	0.563	0.454
VFT	r	−0.087	0.005	0.009	0.906	0.768	−0.823
	p	0.673	0.980	0.963	0.094	0.232	0.177
BNT	r	0.075	0.226	−0.205	0.918	0.916	−0.953
	p	0.715	0.268	0.314	0.082	0.084	**0.047***
TMT-A	r	−0.417	−0.115	0.159	−0.472	−0.974	0.961
	p	0.583	0.885	0.841	0.687	0.147	0.178
TMT-B	r	−0.497	−0.314	0.329	–	–	–
	p	0.503	0.686	0.671	–	–	–
CDT	r	−0.199	−0.109	0.115	0.065	0.560	−0.510
	p	0.319	0.587	0.566	0.935	0.440	0.490
DST	r	0.274	0.236	−0.246	0.789	0.932	−0.939
	p	0.196	0.268	0.247	0.113	**0.021***	**0.018***
SDMT	r	−0.036	−0.126	0.104	–	–	–
	p	0.868	0.559	0.629	–	–	–
ADL	r	0.252	0.305	−0.295	−0.141	−0.306	0.292
	p	0.180	0.101	0.113	0.739	0.461	0.484
CDR	r	0.067	0.022	−0.024	−0.474	−0.344	0.402
	p	0.735	0.913	0.904	0.342	0.504	0.429

Note: Numbers are expressed as mean ± SD, * = $p < 0.05$.

AD = Alzheimer's disease, DLB = Dementia with Lewy body, HC = healthy control.

MMSE = Mini Mental State Examination, MoCA = Montreal Cognitive Assessment, AVLT = Auditory Verbal Learning Test, REY = Rey complex figure test, VFT = Verbal Fluency Test, BNT = Boston Naming Test, TMT = Trail Making Test, CDT = Clock-Drawing Test, DST = Digit Span Test, SDMT = Symbol Digit Modalities Test, ADL = Activity of Daily Living Scale, CDR = Clinical Dementia Rating.

The bold in the table is the corresponding p value when $p < 0.05$.
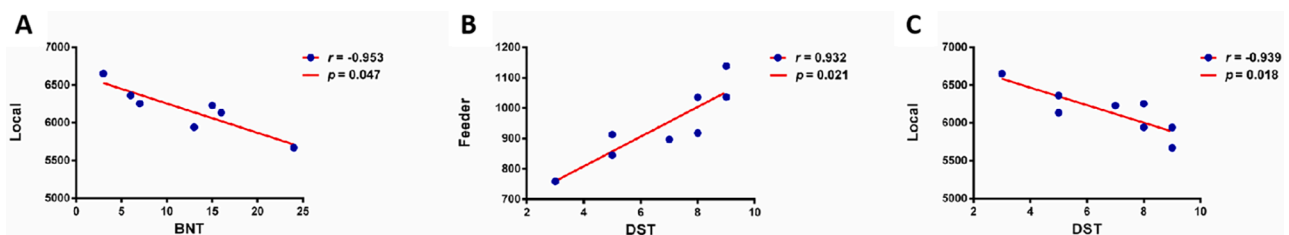
Fig. 7. Correlation analysis between connection strength and clinical characteristics. (A) Correlation between BNT and local connection strength. The BNT score of DLB patients was negatively correlated with local connection strength ($r = -0.953$, $p = 0.047$). (B) Correlation between DST and Feeder connection strength. The DST score of DLB patients was positively correlated with Feeder connection strength ($r = 0.932$, $p = 0.021$). (C) Correlation between DST and local connection strength. The DST score of DLB patients was negatively correlated with local connection strength ($r = -0.939$, $p = 0.018$). Age, sex and GM volume were used as covariates in all partial correlation analyses.

between these central nodes is realized through long-distance paths, which is essential for effective global information transfer in a healthy brain, further reflecting the integration of hubs in a network. Our results show that rich club organization exists in each group of AD, DLB and HC, and ϕ^w_{norm} increases in patients groups, which is consistent with the results of previous studies on rich club coefficient of DTI network in AD patients (Yan et al., 2018; Daianu et al., 2015). This key finding suggests that the changes in information flow in dementia brain networks are not different in quantity but in quality compared with HC. It is different from the previous study which emphasized that the increase of ϕ^w_{norm} in patients at a low level (k < 15) (Yan et al., 2018; Daianu et al., 2015). In our study, when the level of k is higher, the trend of ϕ^w_{norm} increase in

the patient group is more obvious, and there is no difference in the rich club coefficient among the three groups. This may mean that the DLB and AD patients in this study have tighter connections in these central hubs, known as rich club nodes, while sparse local connections between peripheral nodes. In addition, the not completely consistent results may be related to different image modes, node selection and brain network construction. All in all, these results reveal that rich club organization, as a key property of the brain network, is quite stable even in the brain attacked by disease, and is more significant in the highly connected core part. The existence of this organizational structure may provide new evidence for the neural basis of the gradual decline of cognitive function.

4.2. Distribution of rich club nodes and degree comparison based on whole brain among different groups

A large number of studies have emphasized the core role of rich clubs in the whole network structure (Xu et al., 2010). Attacks specifically targeting rich clubs cause about three times as much damage as randomly distributed attacks (Harriger et al., 2012). In this study, it was observed that although the distribution of rich club nodules in the three groups involved frontal, parietal, temporal, occipital and cingulate gyrus, the rich club members in DLB and AD groups changed to varying degrees. Although the brain network rich club organization remained stable in DLB and AD patients, the rich club nodes were significantly reorganized. This suggests that the characteristics of cognitive impairment in DLB and AD patients may be closely related to the destruction and reorganization of rich club nodes in the functional network.

4.2.1. Increased FPN connectivity and decreased SMN connectivity in patients with DLB

In this study, we found that in DLB, the brain regions where the number of rich club nodes significantly increased mainly included the frontal and parietal cortices, corresponding to the previously identified frontal parietal attention network (Fair et al., 2007; Yeo et al., 2011; Dosenbach et al., 2008). The number of rich club nodes in the SMN decreased significantly. FPN is thought to be related to control and attention (Corbetta and Shulman, 2002; Wang et al., 2016). It plays a central role in cognitive control and adaptive execution of task requirements (Cole et al., 2013; Zanto and Gazzaley, 2013). Previous fMRI studies showed that fronto-parietal network abnormalities were associated with DLB cognitive fluctuation (Heitz et al., 2015; Hepp et al., 2013) and visual hallucination (Peraza et al., 2014). In this study, the function enhancement of FPN related nodes may be related to the hub overload and failure theory assumed by Stam (Stam, 2014). The theory holds that in the acute phase, the traffic to the failed node is rerouted to the existing hubs, which will suddenly overload. In the chronic phase, the hub overload can be avoided or compensated by reducing the degree value of "healthy" hubs or the emergence of new hubs. In the process of long-term progressive development, DLB patients gradually appear new hubs in frontal and parietal lobes to compensate for their significant defects in attention and cognitive fluctuations. The decreased function of SMN related nodes may indicate that the brain is more sensitive to the damage of more basic primary sensory function areas that are crucial to individual survival, and more resilient to the damage of higher-order functions (frontal pole and parietal lobe) (Irimia and Van Horn, 2014). This is consistent with the previously reported lower regional homogeneity values in the sensorimotor cortex in DLB group (Peraza et al., 2016). The results of quantitative analysis based on the degree of brain nodes are highly consistent with the above qualitative results about the distribution of rich club nodes. In conclusion, the transfer between high-level cognitive network (FPN) and sensory-motor related networks (SMN and AUD) is the general feature of brain network functional reorganization in DLB patients. This suggests that specific interactions in the network hierarchy topology may play a key role in mediating cognitive impairment (Lee et al., 2013).

In addition, the subcortical rich club nodes in DLB were absent. This finding is consistent with our understanding of the structure and dysfunction of DLB. Compared with the significant cortical atrophy of AD, there is evidence that DLB is more involved in subcortical structures (Watson et al., 2016). For most striatal structures (caudate, putamen, and globus pallidus), volume reduction appears to be more pronounced in DLB than in AD (Pitcher et al., 2012; Whitwell et al., 2008). The decrease of dopamine transporter uptake in basal ganglia revealed by SPECT/PET has been listed as a suggestive biomarker in the diagnostic criteria. All of these are related to parkinsonian dyskinesia in DLB patients (McKeith et al., 2017). All of these are associated with parkinsonian dyskinesia in DLB patients.

Here, we speculate that the transformation and redistribution of hubs between higher cognitive network and sensorimotor network may be an important feature of cognitive compensation in DLB patients. Subcortical network disorders are associated with motor symptoms. These results suggest that by studying the rich club nodes distribution, we can further understand the functional interaction mechanism between brain regions under the influence of DLB.

4.2.2. DMN dysfunction with cerebellar function enhancement in patients with AD

Compared with HC, the number of temporal lobe rich club nodes in AD patients was significantly reduced, involving DMN and AUD. Previous studies have confirmed the presence of AD-related abnormalities in the temporal lobe (Whitwell et al., 2008; Zhou et al., 2008). It may be that the cumulative effect of AD pathological load destroys the rich club connections connecting different functional systems, which may play a role in the cognitive decline observed in patients with AD. In addition, in AD group, some nodes in cerebellar network are identified as rich club nodes. Based on the comparison of the whole brain, it was confirmed from the perspective of quantitative analysis that compared with HC, the nodal degree of bilateral temporal lobe and its adjacent brain regions decreased most significantly in AD patients, while the nodal degree of bilateral midline cortex (left superior frontal gyrus/medial superior frontal gyrus) and cerebellum (bilateral cerebellum area 6, vermis) increased significantly. Interestingly, these decreased and increased brain regions mainly correspond to the left–right and front-back parts of the DMN. DMN is related to various "advanced" cognitive processes (Power et al., 2013). Because of its extensive structural and functional connections with the rest of the brain (Tomasi and Volkow, 2011; Horn et al., 2014), it is thought to act as a "global integrator" in the multimodal integration of information, and may form part of a theorized "global workspace" in order to efficiently transfer information between different functional subunits (Vatansever et al., 2015; de Pasquale et al., 2012; Leech and Sharp, 2014). AD is considered to be a disease of extensive connectivity disorders (Cao et al., 2020). Previous studies have found that cognitive impairment in AD is associated with DMN (Power et al., 2013; Buckner et al., 2008). Combined with the observation that DMN showed the characteristics of brain network reorganization in both directions of weakening and strengthening, we speculated that AD patients may be a dysfunction related to DMN integration mechanism.

Traditionally, cerebellum is related to motor function. It receives sensory inputs from the spinal cord or cortical and subcortical regions and integrates these inputs to fine tune motor activity. Recent studies have shown that cerebellum plays an important role in the evolution of human unique behavior and cognition (Rapoport et al., 2000; Schmahmann and Caplan, 2006; Balsters et al., 2013). The surface area of the cerebellum is 78% of the total surface area of the human neocortex, which accommodates broader connections from the parietal and prefrontal cortex (Sereno et al., 2020). In essence, the cerebellum may be as important as the neocortex, which is the origin of some unique human abilities (such as language, extensive tool making, complex social functions) (Strick et al., 2009; Buckner, 2013). The cerebellum, as a mirror of the brain, plays a compensatory role in the event of brain dysfunction. From the perspective of nodes and networks, our study provides more evidence for the idea that cerebellum and cerebellar networks play a compensatory role in the cognitive progression of AD.

In general, our results tend to suggest that AD is characterized by the long-term injury of ad pathological deposition and structural atrophy, resulting in the decrease of communication between nodes in temporal lobe and the whole brain and the loss of rich club qualification. The frontal and parietal lobes located in the anterior and posterior parts of DMN and the cerebellum with well-preserved structure and function may play a partial compensation role in the disease process.

4.2.3. Distinct node degree and function transfer patterns between DLB and AD

Although both DLB and AD belong to neurodegenerative dementia and have many clinicopathological overlaps, they are, nevertheless, two separate entities. On the whole, AD showed similar node function transfer patterns, whether compared with DLB or HC, that is, the node degree of left and right horizontal distribution decreases and that of front and back vertical distribution increases, but the involved networks are very different. Specifically, in the comparison between DLB and AD, the nodal degree of FPN and DMN around temporal lobe in DLB patients was significantly higher, while the nodal degree of SMN was lower. That the DMN is not markedly hypoactive in DLB patients has been repeatedly reported (Schumacher et al., 2018; Franciotti et al., 2013), which is consistent with our results. In particular, the relative retention of temporal lobe function may be related to the relative preservation of temporal lobe structure in DLB patients. Overall, FPN, SMN, and the peritemporal portion of DMN can be used to distinguish dementia induced by DLB and AD.

4.3. Strengthened communication of rich club organization in patients with DLB and AD

In our study, connection strength was affected by both types of dementia. Compared with HC group, the connection strength of rich club in AD group and DLB group increased significantly, while the feeder and local connection strength of three groups were similar. Our findings suggest that, at least at some point in the progression of dementia, there are stronger rich club connections to facilitate communication throughout the brain. Corresponding to previous studies, it was found that the global rich club communication backbone of early AD is relatively reserved (Daianu et al., 2016; Daianu et al., 2015; Daianu et al., 2015). With the deterioration of cognitive impairment, the correlation between global efficiency and rich club density decreases (Cao et al., 2020). It is speculated that the central area connecting the distal nodes in the rich club may be relatively resistant to the neurodegenerative process (Daianu et al., 2015). Peripheral areas are more vulnerable because of their reduced persistence and lower levels in hierarchical networks (Yan et al., 2018; Stam, 2014). We hypothesized that feeder and local connections are more vulnerable to impairment during the disease course and have a greater impact on cognitive performance, while rich club connections are more robust. When other rich areas are destroyed, due to the compensation mechanism, the brain reorganizes the connections of rich club nodes, thus maintaining a relatively stable brain functional dynamics (van den Heuvel and Sporns, 2011). In addition, some studies have shown that compared with structural connections, functional connections are stronger and more resilient in resisting pathological attacks (Vega-Pons et al., 2016). Furthermore, FC may be less vulnerable and may even act as a compensating mechanism for the loss of structural connectivity in early cognitive decline (Caeyenberghs et al., 2013). However, as the disease gets worse, the damage to feeders and local connections is intensified, and the high-level nodes may also be affected under the condition of continuous load of more information flows, thus leading to the decline of global efficiency (Stam, 2014). But we must point out that this is only one possible explanation. Undoubtedly, a better way to test this explanation would be to conduct longitudinal studies to examine the dynamic effects of plasticity. Taken together, these results suggest that studying the characteristics of rich club connections can provide insight into the functional interactions between brain regions under the influence of DLB and AD.

4.4. Association of connection strength and cognition assessment in DLB patients

Rich club regions are supposed to correspond to one or more resting state networks, and their connections may form the backbone connecting different functional modules in the brain (Zamora-Lopez et al., 2011). It has been noted that synchronization and information transfer between hub regions may contribute to centralized processing and effective integration among multiple cognitive domains (Collin et al., 2014; Crossley et al., 2013). Therefore, the strength of rich club connection may more reflect the overall level of cognitive function. It is worth noting that this study found that with the decrease of rich club connection strength, the cognitive impairment of DLB patients tended to be more obvious (lower score of MOCA). This further supports the view that disruption of the interaction between rich club regions may impair the overall cognition of DLB patients.

At the same time, we observed that the stronger the feeder connection strength was, the weaker the local connection strength was, and the better the attention function (the higher the DST score) of DLB patients was. This may indicate that the ability of local communication and relay integration in the brain of DLB patients to ensure the realization of attention function is disturbed. In addition, the weaker the local connection strength was, and the better the speech assessment (BNT) performance of DLB patients was. This may indicate that the connection of the locally isolated clustering required for naming process is destroyed, and the cross-module integration level based on long-distance connection may play a compensating role to some extent. Previous studies (Yan et al., 2018) have suggested that the loss of connections in peripheral areas (feeder connection and local connection) and rich club areas (feeder connection and rich club connection) may lead to the collapse of global scale network organizations. The persistence of rich club organizations may help explain why the brain has a buffer or reserve capacity to withstand certain changes brought about by aging and disease. With the development of the disease, the rich club areas are affected, and the brain network is more seriously damaged, so that the clinical symptoms are obvious and visible. These views are consistent with our research results.

Surprisingly, no significant correlation was found when assessing connection strength and cognitive performance in patients with AD, suggesting a more complex association between brain connection strength and behavioral performance. Interestingly, although no positive results were captured, we found that the correlation trend between partial cognitive function assessments and connection strength of rich club areas (feeder and rich club) in AD patients was opposite to that in DLB. MoCA, AVLT- delayed recall, REY- delayed recall, VFT and, CDT scores in AD patientsshowed a negative correlation trend with rich club and feeder connection strength, while rich club and feeder connection strength in DLB patients showed a positive correlation trend with the above cognitive function scores. Yet in the absence of a significant correlation, one could propose the following explanation carefully. First, it may be related to the collapse of compensation mechanism. Specifically, DLB patients may also show adaptive network reorganization related to relatively reserved cognitive function (Dubovik et al., 2013). However, these mechanisms are temporary and weakened (Frantzidis et al., 2014). In AD patients, the stronger the connection strength of rich club areas, the worse the cognitive function of AD, that is, the compensatory effect of enhancing the connection strength of the rich club can no longer resist the degree of cognitive decline of the patients, so the patients appear to be unable to make ends meet. Second, it may further indicate that DLB and AD have different dynamic compensation processes, which need further study. In general, our results suggest that this change in measurement may provide a new topological feature for the prediction of cognitive impairment.

5. Limitations

Several limitations are worth noting. First, the sample size is limited, especially for DLB patients with complete cognitive assessment data. However, efforts are being made to recruit more subjects to improve the data, which means that we will use a larger sample size in further studies to prove the validity of these findings. Secondly, many patients are

taking dopamine preparations, cholinergic drugs and other drugs to control their symptoms, making the potential effects of drugs on neural activity difficult to eliminate. Since it is difficult to recruit enough patients who have not taken any drug at the stage of dementia, it is necessary to further study the medication status of dementia patients to verify our results. Third, there is no standard or clear threshold to construct the correlation matrix of functional brain networks, because the results may change according to different network thresholds. Although the results we report in the text are based on a fixed network density, we provide a series of threshold results in the supplementary materials, which are roughly equivalent to the results in the text. Finally, using a cross-sectional design, the causal relationship between abnormal rich club organization and its accompanying changes in network restructuring and disease progression is unclear. In future studies, large sample longitudinal design should be considered to solve this problem.

6. Conclusion

In conclusion, our study found a relatively stable rich club organization with enhanced rich club connectivity in patients with DLB and AD. But there has been a marked change in the membership of their rich club. DLB may lead to functional reorganization from the sensorimotor cortex (SMN) to the higher-order cognitive network (FPN) by affecting the hierarchical structure of the brain network. Patients with AD are potentially affected by brain structural atrophy and show remodeling characteristics of DMN dysfunction and enhanced cerebellar function. More interestingly, we also found that the strength of rich club connection was associated with cognitive assessment in DLB patients. These findings suggest that robust rich clubs and rich club connections may help to maintain stable brain functional dynamics to a certain extent, but the interruption and redistribution of membership in rich club nodes may play a causal role in the symptomatology of DLB and AD. To sum up, rich club organization may provide a new perspective on how DLB and AD affect brain topology and function. It may provide a potential biomarker for the development of more effective therapeutic methods and diagnostic tools to improve clinical management.

CRediT authorship contribution statement

Wen-ying Ma: Writing – original draft, Visualization, Data curation, Investigation. **Qun Yao:** Writing – review & editing, Investigation, Validation. **Guan-jie Hu:** Formal analysis. **Hong-lin Ge:** Formal analysis. **Chen Xue:** Formal analysis. **Ying-ying Wang:** Investigation. **Yi-xin Yan:** Investigation. **Chao-yong Xiao:** Supervision. **Jing-Ping Shi:** Conceptualization, Resources, Project administration. **Jiu Chen:** Conceptualization, Methodology.

Declaration of Competing Interest

The authors declare that they have no known competing financial interests or personal relationships that could have appeared to influence the work reported in this paper.

Appendix A. Supplementary data

Supplementary data to this article can be found online at https://doi.org/10.1016/j.nicl.2021.102930.

References

McKeith, I.G., Boeve, B.F., Dickson, D.W., Halliday, G., Taylor, J.P., Weintraub, D., et al., 2017. Diagnosis and management of dementia with Lewy bodies: Fourth consensus report of the DLB Consortium. Neurology 89, 88–100.

McKeith, I., O'Brien, J., Walker, Z., Tatsch, K., Booij, J., Darcourt, J., et al., 2007. Sensitivity and specificity of dopamine transporter imaging with 123I-FP-CIT SPECT in dementia with Lewy bodies: a phase III, multicentre study. Lancet Neurol 6, 305–313.

McKeith, I.G., Dickson, D.W., Lowe, J., Emre, M., O'Brien, J.T., Feldman, H., et al., 2005. Diagnosis and management of dementia with Lewy bodies: third report of the DLB Consortium. Neurology 65, 1863–1872.

McKeith, I.G., Galasko, D., Kosaka, K., Perry, E.K., Dickson, D.W., Hansen, L.A., et al., 1996. Consensus guidelines for the clinical and pathologic diagnosis of dementia with Lewy bodies (DLB): report of the consortium on DLB international workshop. Neurology 47, 1113–1124.

McKeith, I.G., Fairbairn, A.F., Perry, R.H., Thompson, P., 1994. The clinical diagnosis and misdiagnosis of senile dementia of Lewy body type (SDLT). Br J Psychiatry 165, 324–332.

Daianu, M., Mezher, A., Mendez, M.F., Jahanshad, N., Jimenez, E.E., Thompson, P.M., 2016. Disrupted rich club network in behavioral variant frontotemporal dementia and early-onset Alzheimer's disease. Hum Brain Mapp 37, 868–883.

Sporns, O., Honey, C.J., Kotter, R., 2007. Identification and classification of hubs in brain networks. PLoS One 2, e1049.

van den Heuvel, M.P., Mandl, R.C., Stam, C.J., Kahn, R.S., Hulshoff Pol, H.E., 2010. Aberrant frontal and temporal complex network structure in schizophrenia: a graph theoretical analysis. J Neurosci 30, 15915–15926.

van den Heuvel, M.P., Sporns, O., 2011. Rich-club organization of the human connectome. J Neurosci 31, 15775–15786.

Yan, T., Wang, W., Yang, L., Chen, K., Chen, R., Han, Y., 2018. Rich club disturbances of the human connectome from subjective cognitive decline to Alzheimer's disease. Theranostics 8, 3237–3255.

van den Heuvel, M.P., Sporns, O., Collin, G., Scheewe, T., Mandl, R.C., Cahn, W., et al., 2013. Abnormal rich club organization and functional brain dynamics in schizophrenia. JAMA Psychiatry 70, 783–792.

Ray, S., Miller, M., Karalunas, S., Robertson, C., Grayson, D.S., Cary, R.P., et al., 2014. Structural and functional connectivity of the human brain in autism spectrum disorders and attention-deficit/hyperactivity disorder: A rich club-organization study. Hum Brain Mapp 35, 6032–6048.

Collin, G., Sporns, O., Mandl, R.C., van den Heuvel, M.P., 2014. Structural and functional aspects relating to cost and benefit of rich club organization in the human cerebral cortex. Cereb Cortex 24, 2258–2267.

Collin, G., Kahn, R.S., de Reus, M.A., Cahn, W., van den Heuvel, M.P., 2014. Impaired rich club connectivity in unaffected siblings of schizophrenia patients. Schizophr Bull 40, 438–448.

Crossley, N.A., Mechelli, A., Scott, J., Carletti, F., Fox, P.T., McGuire, P., et al., 2014. The hubs of the human connectome are generally implicated in the anatomy of brain disorders. Brain 137, 2382–2395.

Buckner, R.L., Sepulcre, J., Talukdar, T., Krienen, F.M., Liu, H., Hedden, T., et al., 2009. Cortical hubs revealed by intrinsic functional connectivity: mapping, assessment of stability, and relation to Alzheimer's disease. J Neurosci 29, 1860–1873.

Dai, Z., Yan, C., Li, K., Wang, Z., Wang, J., Cao, M., et al., 2015. Identifying and Mapping Connectivity Patterns of Brain Network Hubs in Alzheimer's Disease. Cereb Cortex 25, 3723–3742.

Brier, M.R., Thomas, J.B., Fagan, A.M., Hassenstab, J., Holtzman, D.M., Benzinger, T.L., et al., 2014. Functional connectivity and graph theory in preclinical Alzheimer's disease. Neurobiol Aging 35, 757–768.

Shu, N., Wang, X., Bi, Q., Zhao, T., Han, Y., 2018. Disrupted Topologic Efficiency of White Matter Structural Connectome in Individuals with Subjective Cognitive Decline. Radiology 286, 229–238.

Daianu, M., Jahanshad, N., Nir, T.M., Jack Jr., C.R., Weiner, M.W., Bernstein, M.A., et al., 2015. Rich club analysis in the Alzheimer's disease connectome reveals a relatively undisturbed structural core network. Hum Brain Mapp 36, 3087–3103.

Zhao, Q.F., Tan, L., Wang, H.F., Jiang, T., Tan, M.S., Tan, L., et al., 2016. The prevalence of neuropsychiatric symptoms in Alzheimer's disease: Systematic review and meta-analysis. J Affect Disord 190, 264–271.

Gu, L., Chen, J., Gao, L., Shu, H., Wang, Z., Liu, D., et al., 2018. Cognitive reserve modulates attention processes in healthy elderly and amnestic mild cognitive impairment: An event-related potential study. Clin Neurophysiol 129, 198–207.

Walker, L., McAleese, K.E., Thomas, A.J., Johnson, M., Martin-Ruiz, C., Parker, C., et al., 2015. Neuropathologically mixed Alzheimer's and Lewy body disease: burden of pathological protein aggregates differs between clinical phenotypes. Acta Neuropathol 129, 729–748.

Ruffmann, C., Calboli, F.C., Bravi, I., Gveric, D., Curry, L.K., de Smith, A., et al., 2016. Cortical Lewy bodies and Abeta burden are associated with prevalence and timing of dementia in Lewy body diseases. Neuropathol Appl Neurobiol 42, 436–450.

Robinson, J.L., Richardson, H., Xie, S.X., Suh, E., Van Deerlin, V.M., Alfaro, B., et al., 2020. The development and convergence of co-pathologies in Alzheimer's disease. Brain.

Montine, T.J., Phelps, C.H., Beach, T.G., Bigio, E.H., Cairns, N.J., Dickson, D.W., et al., 2012. National Institute on Aging-Alzheimer's Association guidelines for the neuropathologic assessment of Alzheimer's disease: a practical approach. Acta Neuropathol 123, 1–11.

Peraza, L.R., Taylor, J.P., Kaiser, M., 2015. Divergent brain functional network alterations in dementia with Lewy bodies and Alzheimer's disease. Neurobiol Aging 36, 2458–2467.

McKhann, G.M., Knopman, D.S., Chertkow, H., Hyman, B.T., Jack Jr., C.R., Kawas, C.H., et al., 2011. The diagnosis of dementia due to Alzheimer's disease: recommendations from the National Institute on Aging-Alzheimer's Association workgroups on diagnostic guidelines for Alzheimer's disease. Alzheimers Dement 7, 263–269.

Tombaugh, T.N., McIntyre, N.J., 1992. The mini-mental state examination: a comprehensive review. J Am Geriatr Soc 40, 922–935.

Horton, D.K., Hynan, L.S., Lacritz, L.H., Rossetti, H.C., Weiner, M.F., Cullum, C.M., 2015. An Abbreviated Montreal Cognitive Assessment (MoCA) for Dementia Screening. Clin Neuropsychol 29, 413–425.

Morris, J.C., 1993. The Clinical Dementia Rating (CDR): current version and scoring rules. Neurology 43, 2412–2414.

Vakil, E., Blachstein, H., 1993. Rey Auditory-Verbal Learning Test: structure analysis. J Clin Psychol 49, 883–890.

Mainland, B.J., Amodeo, S., Shulman, K.I., 2014. Multiple clock drawing scoring systems: simpler is better. Int J Geriatr Psychiatry 29, 127–136.

Bowden, S.C., Petrauskas, V.M., Bardenhagen, F.J., Meade, C.E., Simpson, L.C., 2013. Exploring the dimensionality of digit span. Assessment 20, 188–198.

Bagby, R.M., Ryder, A.G., Schuller, D.R., Marshall, M.B., 2004. The Hamilton Depression Rating Scale: has the gold standard become a lead weight? Am J Psychiatry 161 (12), 2163–2177.

Ma, W.Y., Yao, Q., Hu, G.J., Xiao, C.Y., Shi, J.P., Chen, J., 2019. Dysfunctional Dynamics of Intra- and Inter-network Connectivity in Dementia With Lewy Bodies. Front Neurol 10, 1265.

O'Callaghan, C., Firbank, M., Tomassini, A., Schumacher, J., O'Brien, J.T., Taylor, J.P., 2021. Impaired sensory evidence accumulation and network function in Lewy body dementia. Brain Commun 3 (fcab089).

Schumacher, J., Peraza, L.R., Firbank, M., Thomas, A.J., Kaiser, M., Gallagher, P., et al., 2019. Dynamic functional connectivity changes in dementia with Lewy bodies and Alzheimer's disease. Neuroimage Clin 22, 101812.

Schumacher, J., Taylor, J.P., Hamilton, C.A., Firbank, M., Donaghy, P.C., Roberts, G., et al., 2021. Functional connectivity in mild cognitive impairment with Lewy bodies. J Neurol 268, 4707–4720.

Chen, J., Duan, X., Shu, H., Wang, Z., Long, Z., Liu, D., et al., 2016. Differential contributions of subregions of medial temporal lobe to memory system in amnestic mild cognitive impairment: insights from fMRI study. Sci Rep 6, 26148.

Friston, K.J., Williams, S., Howard, R., Frackowiak, R.S., Turner, R., 1996. Movement-related effects in fMRI time-series. Magn Reson Med 35, 346–355.

Satterthwaite, T.D., Elliott, M.A., Gerraty, R.T., Ruparel, K., Loughead, J., Calkins, M.E., et al., 2013. An improved framework for confound regression and filtering for control of motion artifact in the preprocessing of resting-state functional connectivity data. Neuroimage 64, 240–256.

Yan, C.G., Cheung, B., Kelly, C., Colcombe, S., Craddock, R.C., Di Martino, A., et al., 2013. A comprehensive assessment of regional variation in the impact of head micromovements on functional connectomics. Neuroimage 76, 183–201.

Power, J.D., Cohen, A.L., Nelson, S.M., Wig, G.S., Barnes, K.A., Church, J.A., et al., 2011. Functional network organization of the human brain. Neuron 72, 665–678.

Chai, X.J., Castanon, A.N., Ongur, D., Whitfield-Gabrieli, S., 2012. Anticorrelations in resting state networks without global signal regression. Neuroimage 59, 1420–1428.

Murphy, K., Birn, R.M., Handwerker, D.A., Jones, T.B., Bandettini, P.A., 2009. The impact of global signal regression on resting state correlations: are anti-correlated networks introduced? Neuroimage 44 (3), 893–905.

Lei, D., Li, K., Li, L., Chen, F., Huang, X., Lui, S., et al., 2015. Disrupted Functional Brain Connectome in Patients with Posttraumatic Stress Disorder. Radiology 276, 818–827.

Zhang, Z., Liao, W., Chen, H., Mantini, D., Ding, J.R., Xu, Q., et al., 2011. Altered functional-structural coupling of large-scale brain networks in idiopathic generalized epilepsy. Brain 134, 2912–2928.

Wang, S., Li, Y., Qiu, S., Zhang, C., Wang, G., Xian, J., et al., 2016. Reorganization of rich-clubs in functional brain networks during propofol-induced unconsciousness and natural sleep. Schizophrenia Bulletin 25, 102188.

Rubinov, M., Sporns, O., 2010. Complex network measures of brain connectivity: uses and interpretations. Neuroimage 52, 1059–1069.

Cao, R., Wang, X., Gao, Y., Li, T., Zhang, H., Hussain, W., et al., 2020. Abnormal Anatomical Rich-Club Organization and Structural-Functional Coupling in Mild Cognitive Impairment and Alzheimer's Disease. Oxid Med Cell Longev 11, 53.

Ball, G., Aljabar, P., Zebari, S., Tusor, N., Arichi, T., Merchant, N., et al., 2014. Rich-club organization of the newborn human brain. Proc Natl Acad Sci U S A 111, 7456–7461.

de Reus, M.A., van den Heuvel, M.P., 2013. The parcellation-based connectome: limitations and extensions. Neuroimage 80, 397–404.

Sporns, O., 2011. The human connectome: a complex network. Ann N Y Acad Sci 1224, 109–125.

van den Heuvel, M.P., Mandl, R.C., Kahn, R.S., Hulshoff Pol, H.E., 2009. Functionally linked resting-state networks reflect the underlying structural connectivity architecture of the human brain. Hum Brain Mapp 30, 3127–3141.

Xu, X.K., Zhang, J., Small, M., 2010. Rich-club connectivity dominates assortativity and transitivity of complex networks. Phys Rev E Stat Nonlin Soft Matter Phys 82, 046117.

Harriger, L., van den Heuvel, M.P., Sporns, O., 2012. Rich club organization of macaque cerebral cortex and its role in network communication. PLoS One 7, e46497.

Fair, D.A., Dosenbach, N.U., Church, J.A., Cohen, A.L., Brahmbhatt, S., Miezin, F.M., et al., 2007. Development of distinct control networks through segregation and integration. Proc Natl Acad Sci U S A 104, 13507–13512.

Yeo, B.T., Krienen, F.M., Sepulcre, J., Sabuncu, M.R., Lashkari, D., Hollinshead, M., et al., 2011. The organization of the human cerebral cortex estimated by intrinsic functional connectivity. J Neurophysiol 106, 1125–1165.

Dosenbach, N.U., Fair, D.A., Cohen, A.L., Schlaggar, B.L., Petersen, S.E., 2008. A dual-networks architecture of top-down control. Trends Cogn Sci 12, 99–105.

Corbetta, M., Shulman, G.L., 2002. Control of goal-directed and stimulus-driven attention in the brain. Nat Rev Neurosci 3, 201–215.

Wang, J., Lu, M., Fan, Y., Wen, X., Zhang, R., Wang, B., et al., 2016. Exploring brain functional plasticity in world class gymnasts: a network analysis. Brain Struct Funct 221, 3503–3519.

Cole, M.W., Reynolds, J.R., Power, J.D., Repovs, G., Anticevic, A., Braver, T.S., 2013. Multi-task connectivity reveals flexible hubs for adaptive task control. Nat Neurosci 16, 1348–1355.

Zanto, T.P., Gazzaley, A., 2013. Fronto-parietal network: flexible hub of cognitive control. Trends Cogn Sci 17, 602–603.

Heitz, C., Noblet, V., Cretin, B., Philippi, N., Kremer, L., Stackfleth, M., et al., 2015. Neural correlates of visual hallucinations in dementia with Lewy bodies. Alzheimers Res Ther 7, 6.

Hepp, D.H., da Hora, C.C., Koene, T., Uitdehaag, B.M., van den Heuvel, O.A., Klein, M., et al., 2013. Cognitive correlates of visual hallucinations in non-demented Parkinson's disease patients. Parkinsonism Relat Disord 19, 795–799.

Peraza, L.R., Kaiser, M., Firbank, M., Graziadio, S., Bonanni, L., Onofrj, M., et al., 2014. fMRI resting state networks and their association with cognitive fluctuations in dementia with Lewy bodies. Neuroimage Clin 4, 558–565.

Stam, C.J., 2014. Modern network science of neurological disorders. Nat Rev Neurosci 15, 683–695.

Irimia, A., Van Horn, J.D., 2014. Systematic network lesioning reveals the core white matter scaffold of the human brain. Front Hum Neurosci 8, 51.

Peraza, L.R., Colloby, S.J., Deboys, L., O'Brien, J.T., Kaiser, M., Taylor, J.P., 2016. Regional functional synchronizations in dementia with Lewy bodies and Alzheimer's disease. Int Psychogeriatr 28, 1143–1151.

Lee, H., Mashour, G.A., Noh, G.J., Kim, S., Lee, U., 2013. Reconfiguration of network hub structure after propofol-induced unconsciousness. Anesthesiology 119, 1347–1359.

Watson, R., Colloby, S.J., Blamire, A.M., O'Brien, J.T., 2016. Subcortical volume changes in dementia with Lewy bodies and Alzheimer's disease. A comparison with healthy aging. Int Psychogeriatr 28, 529–536.

Pitcher, T.L., Melzer, T.R., Macaskill, M.R., Graham, C.F., Livingston, L., Keenan, R.J., et al., 2012. Reduced striatal volumes in Parkinson's disease: a magnetic resonance imaging study. Transl Neurodegener 1, 17.

Whitwell, J.L., Shiung, M.M., Przybelski, S.A., Weigand, S.D., Knopman, D.S., Boeve, B. F., et al., 2008. MRI patterns of atrophy associated with progression to AD in amnestic mild cognitive impairment. Neurology 70, 512–520.

Zhou, Y., Dougherty Jr., J.H., Hubner, K.F., Bai, B., Cannon, R.L., Hutson, R.K., 2008. Abnormal connectivity in the posterior cingulate and hippocampus in early Alzheimer's disease and mild cognitive impairment. Alzheimers Dement 4, 265–270.

Power, J.D., Schlaggar, B.L., Lessov-Schlaggar, C.N., Petersen, S.E., 2013. Evidence for hubs in human functional brain networks. Neuron 79, 798–813.

Tomasi, D., Volkow, N.D., 2011. Association between functional connectivity hubs and brain networks. Cereb Cortex 21, 2003–2013.

Horn, A., Ostwald, D., Reisert, M., Blankenburg, F., 2014. The structural-functional connectome and the default mode network of the human brain. Neuroimage 102 (Pt 1), 142–151.

Vatansever, D., Menon, D.K., Manktelow, A.E., Sahakian, B.J., Stamatakis, E.A., 2015. Default Mode Dynamics for Global Functional Integration. J Neurosci 35, 15254–15262.

de Pasquale, F., Della Penna, S., Snyder, A.Z., Marzetti, L., Pizzella, V., Romani, G.L., et al., 2012. A cortical core for dynamic integration of functional networks in the resting human brain. Neuron 74, 753–764.

Leech, R., Sharp, D.J., 2014. The role of the posterior cingulate cortex in cognition and disease. Brain 137, 12–32.

Buckner, R.L., Andrews-Hanna, J.R., Schacter, D.L., 2008. The brain's default network: anatomy, function, and relevance to disease. Ann N Y Acad Sci 1124, 1–38.

Rapoport, M., van Reekum, R., Mayberg, H., 2000. The role of the cerebellum in cognition and behavior: a selective review. J Neuropsychiatry Clin Neurosci 12, 193–198.

Schmahmann, J.D., Caplan, D., 2006. Cognition, emotion and the cerebellum. Brain 129, 290–292.

Balsters, J.H., Whelan, C.D., Robertson, I.H., Ramnani, N., 2013. Cerebellum and cognition: evidence for the encoding of higher order rules. Cereb Cortex 23, 1433–1443.

Sereno, M.I., Diedrichsen, J., Tachrount, M., Testa-Silva, G., d'Arceuil, H., De Zeeuw, C., 2020. The human cerebellum has almost 80% of the surface area of the neocortex. Proc Natl Acad Sci U S A 117, 19538–19543.

Strick, P.L., Dum, R.P., Fiez, J.A., 2009. Cerebellum and nonmotor function. Annu Rev Neurosci 32, 413–434.

Buckner, R.L., 2013. The cerebellum and cognitive function: 25 years of insight from anatomy and neuroimaging. Neuron 80, 807–815.

Schumacher, J., Peraza, L.R., Firbank, M., Thomas, A.J., Kaiser, M., Gallagher, P., et al., 2018. Functional connectivity in dementia with Lewy bodies: A within- and between-network analysis. Hum Brain Mapp 39, 1118–1129.

Franciotti, R., Falasca, N.W., Bonanni, L., Anzellotti, F., Maruotti, V., Comani, S., et al., 2013. Default network is not hypoactive in dementia with fluctuating cognition: an Alzheimer disease/dementia with Lewy bodies comparison. Neurobiol Aging 34, 1148–1158.

Daianu, M., Jahanshad, N., Mendez, M.F., Bartzokis, G., Jimenez, E.E., Thompson, P.M., 2015. Communication of brain network core connections altered in behavioral variant frontotemporal dementia but possibly preserved in early-onset Alzheimer's disease. Proc SPIE Int Soc. Opt Eng 9413.

Daianu, M., Jahanshad, N., Villalon-Reina, J.E., Prasad, G., Jacobs, R.E., Barnes, S., et al., 2015. 7T Multi-shell Hybrid Diffusion Imaging (HYDI) for Mapping Brain Connectivity in Mice. Proc SPIE Int Soc. Opt Eng 9413.

Vega-Pons, S., Olivetti, E., Avesani, P., Dodero, L., Gozzi, A., Bifone, A., 2016. Differential Effects of Brain Disorders on Structural and Functional Connectivity. Front Neurosci 10, 605.

Caeyenberghs, K., Leemans, A., Leunissen, I., Michiels, K., Swinnen, S.P., 2013. Topological correlations of structural and functional networks in patients with traumatic brain injury. Front Hum Neurosci 7, 726.

Zamora-Lopez, G., Zhou, C., Kurths, J., 2011. Exploring brain function from anatomical connectivity. Front Neurosci 5, 83.

Crossley, N.A., Mechelli, A., Vertes, P.E., Winton-Brown, T.T., Patel, A.X., Ginestet, C.E., et al., 2013. Cognitive relevance of the community structure of the human brain functional coactivation network. Proc Natl Acad Sci U S A 110, 11583–11588.

Dubovik, S., Bouzerda-Wahlen, A., Nahum, L., Gold, G., Schnider, A., Guggisberg, A.G., 2013. Adaptive reorganization of cortical networks in Alzheimer's disease. Clin Neurophysiol 124, 35–43.

Frantzidis, C.A., Vivas, A.B., Tsolaki, A., Klados, M.A., Tsolaki, M., Bamidis, P.D., 2014. Functional disorganization of small-world brain networks in mild Alzheimer's Disease and amnestic Mild Cognitive Impairment: an EEG study using Relative Wavelet Entropy (RWE). Front Aging Neurosci 6, 224.